Proceedings of ASME Turbo Expo 2010: Power for Land, Sea and Air
GT2010
June 14-18, 2010, Glasgow, UK

GT2010-22151

CHARACTERISTICS OF MULTI-CAVITY TRAPPED VORTEX COMBUSTORS

Alejandro M. Briones
University of Dayton Research Institute
Dayton, OH, USA

Balu Sekar
Air Force Research Laboratory
WPAFB, OH USA

ABSTRACT

This research is motivated towards improving and optimizing the performance of AFRL's Inter-Turbine Burner (ITB) in terms of greater combustion efficiency, reduced losses and exit temperature profile requirements. The ITB is a mini-combustor concept, situated in between the high and low pressure turbine stages and typically contains multiple fueled and non-fueled Trapped Vortex Combustor (TVC) cavities. The size, placement, and arrangement of these cavities have tremendous effect on the combustor exit temperature profile. The detailed understanding of the effect of these cavities in a three-dimensional ITB configuration would be very difficult and computationally prohibited. Therefore, a simple but somewhat similar conceptual axi-symmetric burner is used here the design variations of Trapped Vortex Combustor (TVC) through modeling and simulation. The TVC can be one single cavity or can be represented by multi-cavity combustor. In this paper, both single cavity TVC and multi-cavity TVCs are studied. The single cavity TVC is divided into multiple cavities while the total volume of the combustor remains constant. Four combustors are studied: Baseline, Staged, Three-Staged, and Interdigitated TVC. An extensive computational investigation on the characteristics of these multi-cavity TVCs is presented. FLUENT is used for modeling the axisymmetric reacting flow past cavities using a global eddy dissipation mechanism for C_3H_8-air combustion with detailed thermodynamic and transport properties. Calculations are performed using Standard, RNG, and Realizable k-ε RANS turbulence models. The numerical results are validated against experimental temperature measurements on the Base TVC. Results indicate that the pressure drag is the major contributor to total drag in the Base TVC. However, viscous drag is still significant. By adding a concentric cavity in sequential manner (i.e. Staged TVC), the pressure drag decreases, whereas the viscous drag remains nearly constant. Further addition of a secondary concentric cavity (i.e. Three-Staged TVC), the total drag does not further decrease and both pressure and viscous drag contributions do not change. If instead a non-concentric cavity is added to the Base TVC (i.e. Interdigitated TVC), the pressure drag increases while the viscous drag decreases slightly. The effect of adding swirl flow is to increase the fuel-air mixing and as a result, it increases the maximum exit temperature for all the combustors modeled. The jets and heat release contribute to increase pressure drag with the former being greater. The fuel and air jets and heat release also modify the cavity flow structure. By turning off the fuel and air jets in the Staged TVC, lower drag (or pressure loss) and exit temperature are achieved. It is more effective to turn off the fuel and air jets in the upstream (front) cavity in order to reduce pressure losses. Based on these results, recommendations are provided to the engineer/designer/modeler to improve the performance of the ITB.

NOMENCLATURE

CC	=	Circular cavity
CIC	=	Cavity in cavity
CRV	=	Curved radial vane
H	=	Cavity height
H_{CDF}	=	Height of cavity downstream face
H_{CUF}	=	Height of cavity upstream face
ITB	=	Inter-turbine burner
L	=	Cavity length
RVC	=	Radial vane cavity
SCV	=	Steady cavity vortex
SRV	=	Straight radial vane
TVC	=	Trapped vortex combustor
UCC	=	Ultra-compact combustor
UCV	=	Unsteady cavity vortex
WBF	=	Wake backflow
C_D	=	Drag coefficient
$C_{D,P}$	=	Pressure drag coefficient
$C_{D,v}$	=	Viscous drag coefficient
ϕ_{CAV}	=	Cavity equivalence ratio
ϕ_{GBL}	=	Global equivalence ratio

1. INTRODUCTION

Major advances in combustor technology are required to meet the conflicting challenges of improving performance,

increasing durability, reducing weight, lowering emissions, and maintaining cost. A novel approach proposed by Air Force Research Laboratory (AFRL) [1,2] is the development of the Ultra Compact Combustor (UCC), which can be used to increase the efficiency of the Brayton cycle through reheating [3]. A secondary burner with novel conceptual designs in between the turbine stages within the turbine engine can produce a much more favorable trade-off between specific thrust and thrust specific fuel consumption. The same burner can be used as a main burner as well. However, the implementation of a reheat burner is very challenging in the aerospace industry because jet engines have much stricter weight requirements as compared to land-based gas turbine engines. The increased size and weight incurred from additional engine components could surpass the benefits of increased engine efficiency. Therefore, the reheat combustor must be much shorter than conventional combustors. A shorter burner, however, decreases the residence time leading to excessive unburned fuel leaving the combustor and possibility of damaging the downstream turbine blades may happen, depending upon the residence time of the combustor for the operating fuel-air ratio. These issues are currently being addressed in the AFRL's UCC which incorporates the primary, intermediate, and dilution zones (of conventional combustors) into a much smaller footprint using compressor and turbine features that enable a shorter and potentially less complex gas turbine operating as an inter-turbine burner (ITB) between the high- and low-pressure turbines in a reheat cycle engine.

A schematic of the current ITB is shown in Figure 1. The main air (or vitiated) flow enters the combustor and flows around the bullet nose of the center body. The turning vanes (shown in red) simulate the swirl that would be coming from the compressor rotor in a real gas turbine engine. The flow from the trailing edge of these turning vanes impinges on the turbine inlet guide vanes (IGV) (shown in blue). The function of the IGV is the same as that of a conventional gas turbine engine and they are also referred, in the context of the UCC, as curved radial vanes (CRV). Additional air is admitted through 24 holes equally spaced around the CC and angled at 45° to the radial direction to promote high swirl in the cavity. A small cavity-in-cavity (CIC) that is located on the outer radius of the CC allows fuel-rich spray and injection of fuel and air, respectively, into the CC. Aligned with this cavity, on each CRV, there is a radial vane cavity (RVC) that extends to the center body. Fuel-rich combustion occurs in the CC and flame stabilization occurs as combustion products are re-circulated in the CC. The CC is analogous to a centrifuge; hence, cold nonreactive fuel-air mixture migrates radially outward, while hot reacted mixture migrates radially inward. The cold mixture remains in the CC for a longer period of time to evaporate, mix, and burn. The large density gradient in the cavity along with the high-g flow enhances mixing of cold and hot mixtures creating a very well-mixed combustion zone. The intermediate products of combustion are transported by lower wake pressures into the RVC where combustion continues at a fuel-lean equivalence ratio (ϕ) as the mainstream air is entrained into the wakes. Consequently, combustion primarily takes place in the engine circumferential direction rather than in the axial direction as is conventionally done.

Numerous design variations of the selected configurations have been evaluated, leading to improved configurations with short and efficient flames [4,5,6,7,8,9,10]. Lin et al. [4] showed that in the ITB with straight radial vane (SRV) cavity the combined use of the V-gutter and the RVC provides the best mixing compared to the ITB without both V-gutter and RVC and that of the ITB without V-gutter. This optimum configuration also leads to temperature exit profile much closer to parabolic type of profile and results in reduced maximum temperature. In addition, although the CRV does not reach the flame stability performance of previously conducted experiments on straight radial vane (SRV) tests [5] the CRV exhibits better ITB exit temperature profile than the SRV [6]. Moreover, Thornburgh et al. [7,8] showed that, in the case of ITB with both CRV and RVC, the temperature gradients at high equivalence ratios are much greater than that at lower equivalence ratios. Nevertheless, the addition of driver air jets in the CIC increase exit temperature profile uniformity by enhancing mixing. Furthermore, Sekar et al. [9] showed that for the ITB with CRV and RVC the exit temperature profile for small CC is more sensitive to fuel injection temperature than that for a larger CC, especially in the region near the outer wall of the CC. Even though the extensive experimental and numerical investigations during the past years have led to an optimized ITB a major design problem still persist. Despite the fact that the exit temperature profile has been improved it is still not satisfactory for the range of operating conditions [5-10]. Attainment of the desired temperature profile is of paramount importance because an adverse temperature profile can damage the turbine blades and deteriorate turbine performance. Since stresses are highest at the turbine hub and seal materials need to be protected at the turbine blade tip the temperature profile needs to be parabolic for modern high-performance engines [11].

As discussed above the ITB contains several cavities (i.e. CIC, CC, and RVC) and the size, placement, and arrangement of these cavities have tremendous effect on the exit temperature profile. Consequently, it is important to fundamentally understand the characteristics of multi-cavity combustors in order to provide insights for the optimization of the ITB design. The detailed understanding of the effect of these cavities in a three-dimensional ITB model would be very difficult and computationally prohibited because of the large number of physical events such as evaporation, turbulent mixing, and combustion, and possible cavity configurations [12]. Therefore, a simple but somewhat similar burner is used here for modeling and simulation. We start this investigation by modeling and simulating the baseline trapped-vortex combustor (TVC) [13] since it is better understood and is simpler to model and a limited experimental data exists. This Base TVC is modeled and as well is further split in multiple cavities whereas the volume of the combustor remains constant in order to emulate the ITB multiple cavities.

The purpose of this investigation is to understand the effect of multiple cavity combustors on the flow field in order to provide insights for improvement of the ITB design. The specific objectives are the following. Firstly, we want to examine the flow characteristics of multi-cavity TVCs. Although there is a vast number of publications regarding flow/flame characteristics on single axisymmetric [14,15,16] and planar [17,18,19,20,21] cavities there are (to the best of our knowledge) only two investigations in the literature concerning flow past an arrangement of cavities [22,23]. Mair [22] showed experimentally that the drag of an axisymmetric body with blunt base can be substantially reduced (~35%) by mounting a disk of smaller diameter behind the body. Further reduction (~55%) is achieved with two disks. Molki and Faghri [23] numerically studied the interaction between a buoyancy-induced flow and an array of annular cavities with heat generated from the spindle. The larger the number of cavities the more uniform high-temperature zone adjacent to the finned area was observed. Secondly, we will assess the effect turbulence models on the flow field characteristics because previous investigations on the ITB have only used Realizable k-ε RANS turbulence model [4,6-9]. This is important in order to correct and improve future numerical modeling of the ITB. Thirdly, because the ITB exhibits high swirling flow (cf. Figure 1) axisymmetric swirl flows are also modeled for multi-cavity TVCs to examine its effect on the flow/flame characteristics. Here again, we use several RANS models to assess their effect on the flow/flame characteristics. Finally, we will examine the effect of fuel and air injection on the flow/flame characteristics of multi-cavity TVCs.

2. PHYSICAL-NUMERICAL PROCEDURE

A. GAS PHASE NUMERICAL MODEL

Fluent software is used to simulate the gaseous flow field. For all conditions investigated here the flow Mach number is below 0.13 and the axisymmetric governing equations of continuity, momentum, energy, and turbulence are solved using the segregated pressure-based solver. The Standard, RNG, and Realizable k-ε models are used to simulate the turbulent flow field. The governing equations are discretized using second-order upwind scheme. The gradients and derivatives of the governing equations are computed using the Green-Gauss Node-Based method [24] which is second-order spatially accurate. The pressure values at the faces are obtained by interpolating the pressure from the cell nodes (i.e. the pressure interpolation is a second-order scheme). The pressure-velocity coupling is achieved by using the SIMPLE algorithm. The algebraic multigrid (AMG) scheme is used to solve the discretized governing equations.

B. THERMODYNAMIC AND TRANSPORT PROPERTIES

The thermodynamic and transport properties appearing in the governing equations are temperature and species dependent. The mixture density is computed using the ideal gas law assuming that the pressure remains constant in the flow field at 101,325 Pa. The specific heat capacity of individual species is computed with piecewise polynomials [13]. The viscosity, thermal conductivity, and binary diffusivity of the individual species were based on kinetic theory [25]. Whereas the mixture viscosity and thermal conductivity are computed using the Wilke semi-empirical formulas [26], mixture-averaged formulation is used to compute species diffusivities that are used in the governing equations. The Wilke semi-empirical correlations are used because they apply to non-polar low density gases; hence, these correlations are useful in our investigation. The mixture-averaged diffusivity is a particularly useful simplification when all species, but one, are not abundant. For instance, the mass fraction of N_2 is ~0.72. The formulation used for the calculation of individual and mixture properties is a common practice utilized in many in-house source codes [27] and commercial codes [28,29].

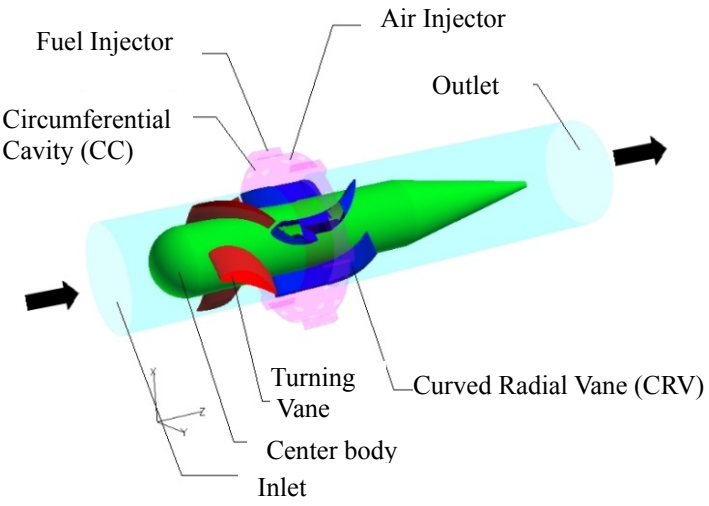

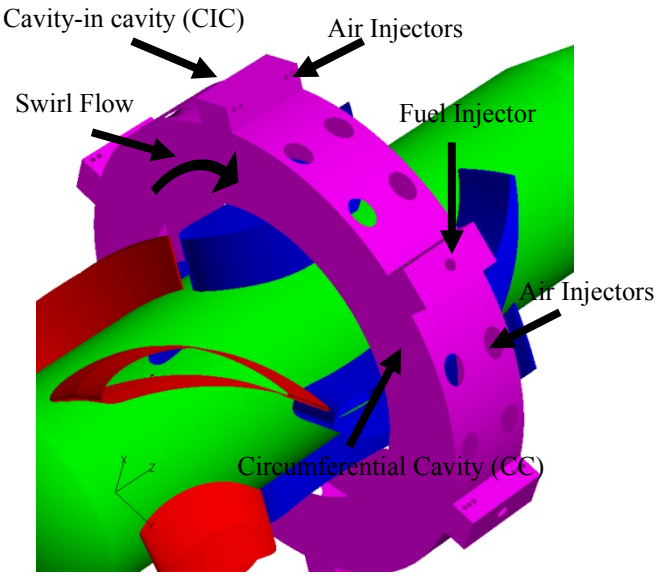

Figure 1. Inter-Turbine Burner (ITB). The inlet, hub, guide vane, blade, circumferential cavity, outlet, cavity-in cavity (CIC), air injectors and fuel injectors are indicated. The swirl flow is also indicated by the bent arrow on the circumferential cavity.

C. COMBUSTION MODEL

In general, numerical modeling of the combustion process requires detailed and/or reduced chemical reaction mechanisms for adequate accuracy. In the present study, propane chemistry is modeled by using a simplified one-step irreversible chemical reaction scheme given below as:

$$C_3H_8 + 5\ O_2 + 5{\times}3.76\ N_2 \rightarrow\ 3\ CO_2 + 4\ H_2O + 5{\times}3.76\ N_2$$

An eddy-dissipation approach was used to account for turbulence-chemistry interaction since in the complicated ITB configuration it is impossible to include even a reduced multi-step, several species chemistry. It is important to note that the purpose of utilizing a single reaction step at this point of the TVC technology evaluation is to simplify the CFD computations and obtain overall global combustion features in the multi-cavity TVCs such as finite-rate flame length, combustion heat release, and TVC exit profiles.

D. GEOMETRY AND MESH

The multi-cavities (Staged, Three-Staged and Interdigitated TVCs) are designed to replicate the same volume of the original cavity in the baseline (Base TVC) taking into consideration the axisymmetric nature of the configuration. Interdigitated fuel and air injection schemes are typically used in high speed and rocket combustion. The basic idea of using this Interdigitated combustor is to penetrate the fuel more into the cross-stream air and provide greater mixing, thereby, achieving uniform temperature distribution in a lean mode of stage of combustion operation [30]. This is usually done by injecting the fuel-air mixture from the cavities, both from the upper and lower wall of the combustion chamber in a staggered mode and this mode of combustion is highly prevalent in the rocket combustion chamber. The Interdigitated, thus, having a lesser cross-sectional area split in the top cavity is not adequate for providing fuel and air injections. Therefore, the total fuel and air is administered in the lower cavity only. Gambit software was used for geometry and mesh generation. Schematics of the four multi-cavity TVC's computational domains with boundary conditions are presented in Figure 2. All geometries were meshed using the structured Map meshing scheme with quadrilateral elements. For a given simulation static mesh adaption was used for regions where scalars exhibited large gradients. The enhanced wall functions [31] are used to resolve the viscous laminar sub-layer. y+ at the wall-adjacent cells is always less than 5 and there are at least more than 10 cells in the viscosity-affected near-wall boundary in order to resolve the mean velocity and turbulent quantities in this region.

E. OPERATING CONDITIONS

For all the TVCs the mainstream inlet annular velocity is 42 m/s and the inlet temperatures are always at 300 K. All wall boundary conditions for all TVCs are assumed to be adiabatic. The cavity air jets are always injected at 12 m/s while the fuel jet is injected at 5 m/s for all the simulations and all TVCs. All TVCs in Figure 2 have the same volume. Similarly, the total fuel and air mass flow rates into the cavities are kept constant. Consequently, the global (ϕ_{GBL}) and local (ϕ_{CAV}) cavity equivalence ratios are kept constant at 0.21 and 4.4, respectively. For instance, the single cavity of the Base TVC, the two cavities of the Staged TVC, the three cavities of the Three-Staged TVC, and the first cavity (from left to right) of the Interdigitated TVC have same ϕ_{CAV}. This is accomplished by reducing the annular jet cross-sectional area as the number of cavities increase. As mentioned before, the second cavity of the Interdigitated TVC has no fuel and air injections since it is not possible to model these jets because in order to keep ϕ_{GBL} and ϕ_{CAV} constant the jets cross-sectional area (and thus annular slot's height) would be very small compared to the overall computational domain. Since fuel and air jets always have the same velocities, the momentum of the individual jets is also kept constant. Moreover, Table 1 shows the aspect ratios or height to length ratios of the various cavities within the multi-cavity TVCs. By splitting the cavity of the Base TVC the height to length ratio increases for all combustors except for the downstream cavity of the Interdigitated TVC.

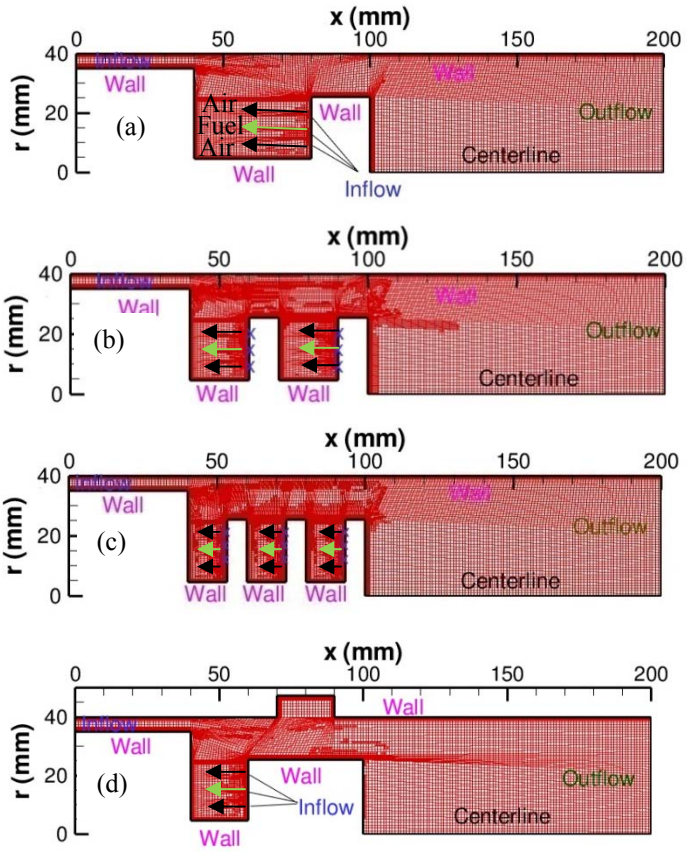

Figure 2. Schematic of the various combustors: (a) Base TVC, (b) Staged TVC, (c) Three-staged TVC, and (d) Interdigitated TVC. The boundary conditions are indicated. The fuel injections are located at the cavity downstream faces, indicated with inflow and with (blue) x (for the Staged and Three-staged TVCs). The inner and outer jets are for air injections (indicated with black arrows), whereas the middle jet is for fuel injection (indicated with light green arrow).

Table 1. Cavity height to length ratio for the various cavities within the multi-cavity TVCs. H_{CUF} and H_{CDF} are the height based on the cavity upstream and downstream face, respectively. H is the height of the remaining cavities which have same upstream and downstream face heights. L is the length of the cavity.

	First or Main Cavity		**Other Cavities**
Combustor	H_{CUF}/L	H_{CDF}/L	H/L
Base TVC	0.76	0.52	-------
Staged TVC	1.53	1.05	1.05
Three-staged TVC	2.29	1.57	1.57
Interdigitated TVC	1.53	1.05	0.36

3. RESULTS AND DISCUSSION

A. VALIDATION OF NUMERICAL MODEL

The validation rig test configuration is shown in Figure 3. This is an axisymmetric configuration and has cavity injection of air and gaseous propane fuel at selected points in the disk. However, in these simulations, for simplicity, the air and fuel injection holes are modeled as a slit with the same amount of mass flow rate of injected air and fuel flow, as that of experiments in Ref. 32. The comparison between numerical simulations and measurements are shown in Figure 3. Appropriate grid discretization and very similar boundary conditions, as discussed earlier were set and are the same as in Ref. 32. Single step propane/air chemistry and the eddy dissipation model were chosen. The calculated radial temperature distributions inside the Base TVC (cf. Figure 2(a)) at several axial stations a) x = 45 mm, b) x = 65 mm, and c) x = 80 mm for $\phi_{CAV} = 4.4$ are shown in Figure 3.

Figure 3 shows the calculated radial temperature profiles in the cavity against experiments at selected axial stations, namely at x = 45, 65, and 80 mm, in which the fuel propane and air are injected. The comparisons show very poor agreement at stations very close to the side of the wall at x = 65 and 80 mm. Overall it is seen that the RNG k-ε RANS model performed better than the Standard and Realizable counterparts. Near the fuel injection, the comparisons tend to be poor due to a possibility of exercising the eddy dissipation global chemistry model for the propane chemistry.

B. FLOW CHARACTERISTICS OF MULTI-CAVITY TRAPPED VORTEX COMBUSTORS

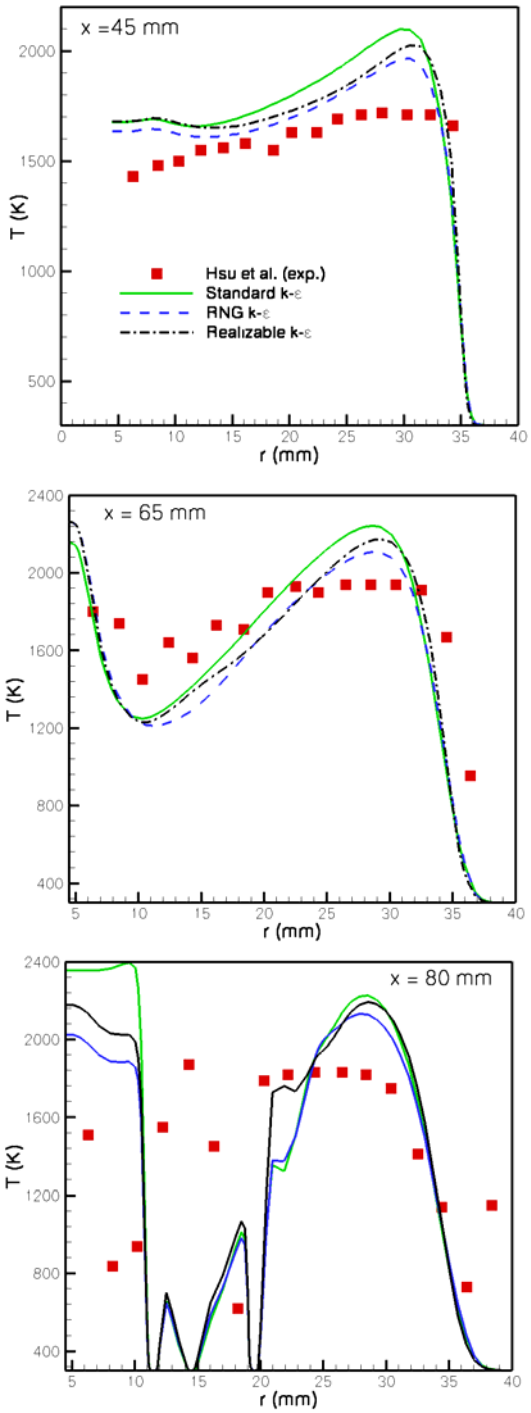

Figure 3. Radial temperature profiles for the Base TVC. The numerical simulations are compared with the measurements of Hsu et al. [32]. The Standard, RNG, and Realizable k-ε RANS turbulence models are used for comparison with measurements.

Now it is worth discussing the flow stabilization criteria in a single cavity because it provides insights into flow/flame stabilization in multi-cavity TVCs. Little Jr. and Whipkey [14] identified three regimes associated with drag. These are the Wake Backflow (WBF), Unsteady Cavity Vortex (UCV), and

the Steady Cavity Vortex (SCV) regime. These three regimes are depicted in Figure 4. In the WBF, flow downstream the afterbody spills upstream into the cavity and the cavity exhibits vortex edge velocity in opposed direction to the mainstream velocity with high-drag coefficient. By moving the afterbody disk downstream from where WBF regime exists, the flow in the cavity transitions to the UCV regime. The cavity exhibits a vortex edge velocity in the same direction as the mainstream flow and the wake backflow does not move upstream past the afterbody disk. The drag coefficient (C_D) fluctuates from low- to high-drag condition. When the disk is positioned at its optimum from the forebody, the flow in the cavity is said to be in the SCV regime. Here the vortex rotates (with edge velocity) in the same direction as the mainstream velocity, fits the cavity nearly perfectly, mass transfer into or out of the cavity is minimum, there is no backflow, and is characterized by low drag. Their cavity optimization criterion [14] was based that in order to reduce C_D, the afterbody disk needs to be large enough to separate the wake backflow from the cavity flow so that a locked vortex can exist in the cavity. Therefore, with the proper choice of cavity dimensions vortices in the cavity can be made stationary. However, a steady vortex yields minimum mass exchange between the vortex and the main flow, which in the TVCs, means that additional air most be supplied within the cavity for combustion to be sustainable.

Figure 6 clearly shows that C_D decreases from Base to Staged TVC when computed with Standard, RNG, and Realizable k-ε RANS models. The Base TVC (cf. Figure 5) is initially operating at somewhat similar condition to that of the SCV regime (cf. Figure 4) since it only exhibits one single dominating vortex with edge velocities in the same direction as the mainstream flow. The total cavity drag coefficient, which viscous drag is negligible, is 0.84 (cf. Figure 7) corresponding to 39 % of total drag and 45 % of pressure drag. The combustor can walls contribute to 78 % of the total viscous drag. The forebody and disk thickness contributes to 22 % of the total viscous drag. Moreover, the first cavity (from left to right) of the Staged TVC exhibits a single dominating vortex, which does not entirely fits inside the cavity, with edge velocities in the same direction as the mainstream. This cavity flow resembles the UCV flow regime (cf. Figure 4). The first cavity drag coefficient is 0.68 corresponding to 36 % of total drag and 44 % of pressure drag (cf. Figure 7). The second cavity does not exhibit a dominating vortex and instead the fuel and air jets impinge on the cavity upstream wall and then mix with the mainstream flow. The second cavity drag coefficient is 0.03 (cf. Figure 7) corresponding to 1.5 % of total drag and ~ 2 % of pressure drag. Although the first cavity exhibits UCV flow structure instead of SVC it contributes to ~50% of total drag reduction, whereas the downstream face of the second disk contributes to the other ~ 50 %. Therefore, all drop in C_D comes from $C_{D,P}$.

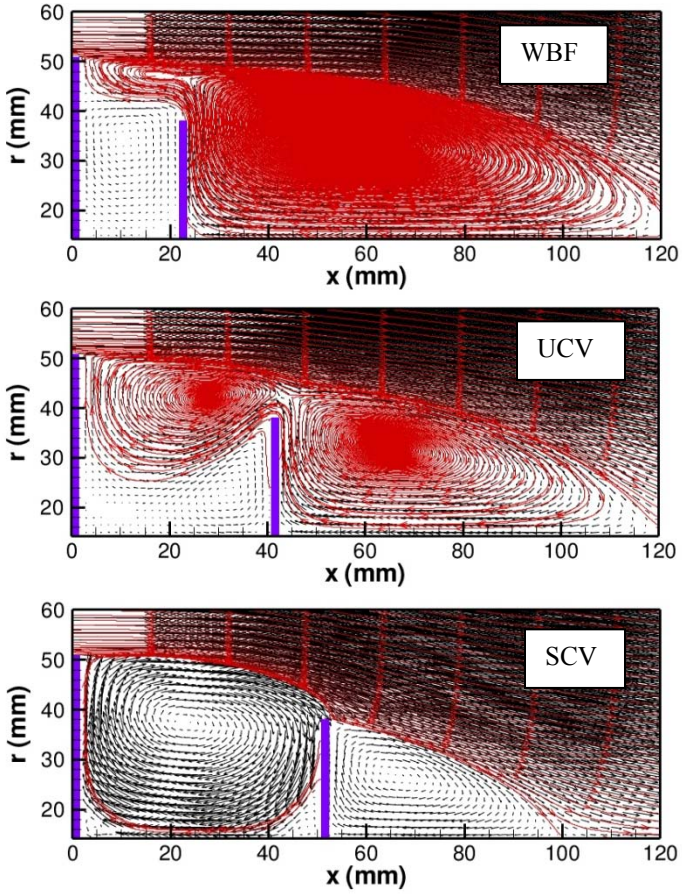

Figure 4. Velocity vectors for an afterbody disk placed at x/D_o=0.2 (WBF), 0.4 (UCV), and 0.5 (SCV) from Ref. 21. The calculations were performed using the Standard k-ε RANS model. The velocity vector lengths are scaled with magnitude. The streamlines are indicated in red.

There is none or negligible decrease in C_D from the Staged to the Three-Staged TVC. Only the Realizable k-ε RANS reports a negligible decrease. The Three-Staged TVC exhibits characteristics of both WBF and UCV flow regimes. The first cavity still exhibits a dominating vortex with edge velocities in the same direction of the mainstream flow. This cavity also exhibits backflow from the second cavity which is characteristic of WBF regime. The first cavity drag coefficient is 0.68 corresponding to 36 % of total drag and 44 % of pressure drag (cf. Figure 7). The second and third cavity flows are very different from the first one, but alike between them. They exhibit flow structures more similar to the UCV and/or SVC. The second and third cavity drag coefficient is 0.02 corresponding to 1 % of total drag and ~ 1 % of total pressure drag (cf. Figure 7). Although the first cavity exhibits characteristics of both WBF and UCV it contributes to ~ 50% of total drag reduction from the Base TVC, whereas the downstream face of the third disk contributes to the other ~ 50 %.

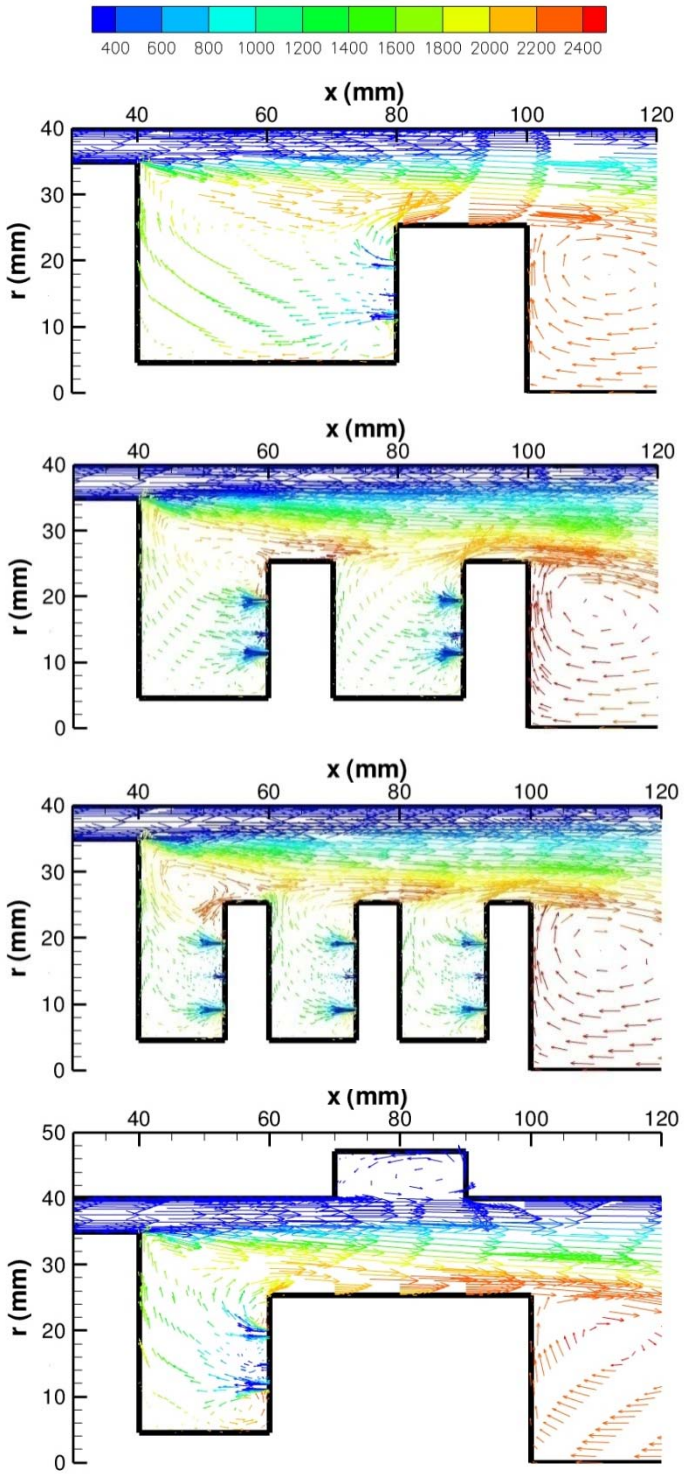

Figure 5. Velocity vectors for Base, Staged, Three-Staged, and Interdigitated TVCs. The calculations were performed using the RNG k-ε RANS model. The velocity vector lengths are scaled with magnitude and colored with temperature in Kelvin.

For the Base, Staged, and Three-Staged TVC $C_{D,V}$ remains nearly constant since the outer combustor wall (i.e. can) does not experience any change in geometry (cf. Figure 6). Nevertheless, for the Interdigitated TVC $C_{D,V}$ decreases due to a reduction in the mainstream flow wetted area. The total drag for this combustor increases due to an increase on $C_{D,P}$. The first and second cavity (from left to right) exhibit similar structures to that of the SCV flow regime. The first cavity drag coefficient is 0.85 similar to that of the Base TVC and corresponds to 37 % of total drag and 42 % of pressure drag (cf. Figure 7). The second cavity drag coefficient is 0.13 corresponding to 6 % of total drag and 7 % of pressure drag (cf. Figure 7). The outer walls contribute to 76 % of the total viscous drag. The second cavity contributes to ~ 72 % increment in pressure drag from the Base TVC, whereas the downstream face of the afterbody disk contributes to ~ 28 % increase in pressure drag.

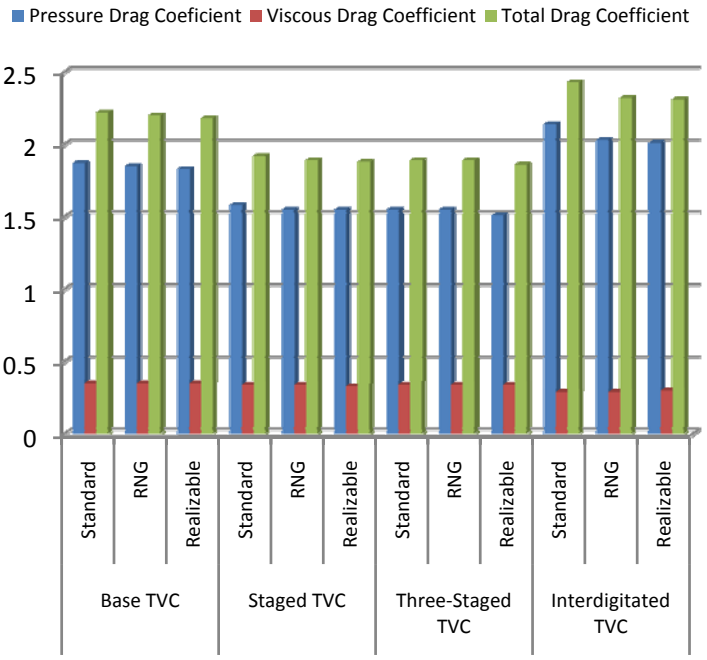

Figure 6. Pressure ($C_{D,P}$), viscous ($C_{D,V}$), and total drag (C_D) coefficients for the Base, Staged, Three-Staged, and Interdigitated TVCs computed using the Standard, RNG, and Realizable k-ε RANS turbulence models.

To further understand why the Staged and Three-Staged TVCs exhibit lower $C_{D,P}$ in comparison with the Base TVC Figure 8 presents the normalized area-averaged total pressure as a function of axial distance for the various TVCs in the context of Figure 5. For all TVCs the total pressure first decreases from the inlet. Then it decreases abruptly indicating flow separation at the forebody. For the Staged and Three-Staged TVC this drastic decrease in total pressure is not as severe as that for the Base and Interdigitated TVCs. Within the cavity the total pressure flattens for the Base TVC. The total pressure then increases in the region near the upstream face of

the afterbody disk and starts to decrease again at the afterbody downstream face. As the flow travels downstream the total pressure increases again. Therefore, the effect of Staged and Three-Staged TVCs is to create total pressure local peaks at each of their cavities and, consequently, pressure loss recovering occurs. This in turn reduces the drag as is shown in Figure 6. Furthermore, the Interdigitated TVC also creates these local peaks of total pressure. However, it is not efficient in recovering the pressure losses due to its initial pressure drop during separation. Therefore, only consecutive concentric cavities can reduce the pressure losses and drag and consecutive non-concentric cavities attenuate pressure losses and drag.

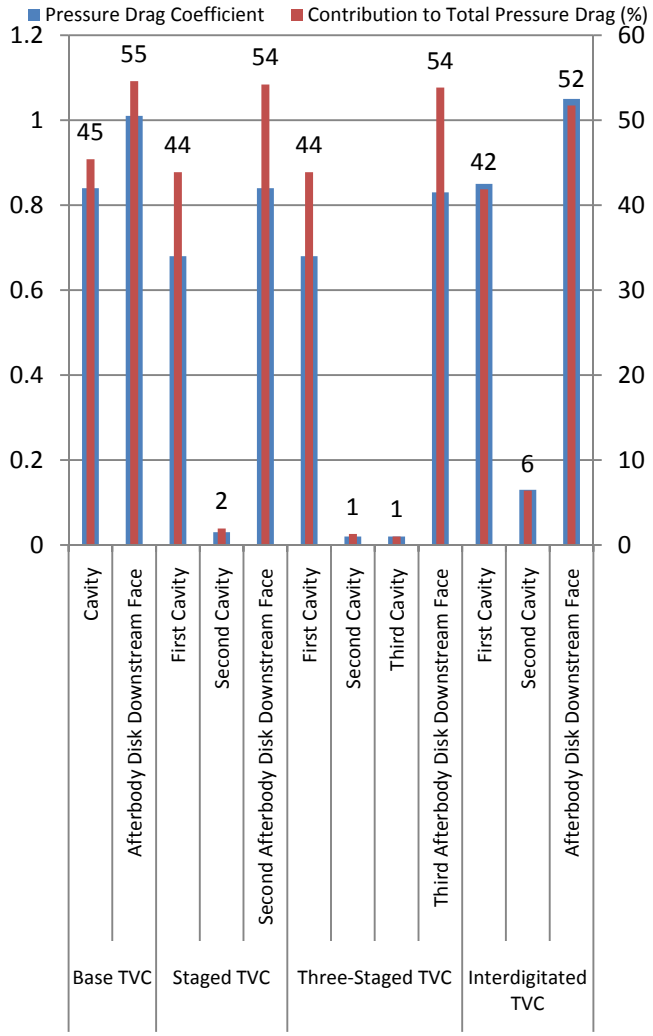

Figure 7. Individual pressure drag coefficients of the various components of the combustors and individual contributions to total pressure drag. Results based on the RNG k-ε RANS model.

Figure 9 presents the outlet radial temperature profiles for the Base, Staged, Three-Staged, and Interdigitated TVCs. Calculations were performed using the Standard, RNG, and Realizable k-ε RANS turbulence models. The four combustors exhibit parabolic temperature profiles which are optimum conditions for gas turbine operation. The Three-Staged TVC exhibits slightly larger maximum exit temperature in comparison with the other combustors. Overall the Staged and Base TVC exhibit the lowest maximum exit temperature. The results obtained using the Standard, RNG, and Realizable are not significantly different.

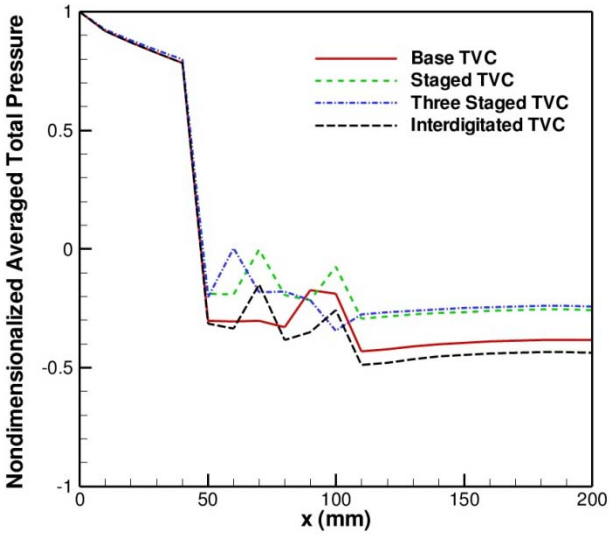

Figure 8. Normalized area-averaged total pressure as a function of axial distance for the various TVCs in the context of Figure 5.

C. EFFECT OF SWIRL FLOW ON MULTI-CAVITY TRAPPED VORTEX COMBUSTORS

From the investigation of Quaale et al. [33] in which circumferential velocities in the ITB from 20 to 45 m/s are reported a characteristic swirl angular velocity of 400 rad/s is used. Figure 10 presents the exit temperature profiles for the non-swirled (lines) and swirled (lines and symbols) combustors discussed in the context of Figure 9. In addition, all calculations were performed using the Standard, RNG, and Realizable k-ε RANS turbulence models. There are several important observations from this figure. First, in descending order the Realizable predicts higher temperature than the RNG and Standard models. Second, the effect of swirl is to enhance hot products mixing with cold mainstream air increasing the exit temperature. Fourth, the increase in temperature corresponds to an increase in combustion efficiency that is less 1 %. The combustion efficiency of all combustors is near to 100 %. Therefore, the temperature, especially, that of the swirled TVCs should correspond to that of a canonical strained diffusion flame. Finally, the increase in temperature is not capture by the Standard model and, consequently, it should not be use for swirled flows. Surprisingly, the Realizable model predicts the increase in temperature as the RNG model does.

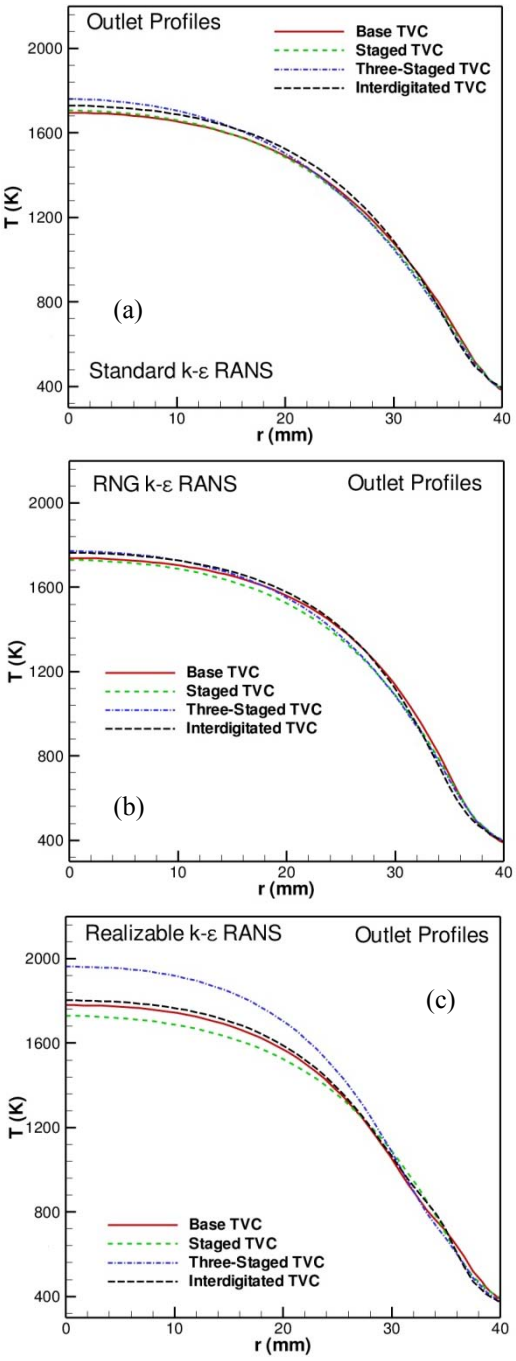

Figure 9. Outlet radial temperature profiles for the Base, Staged, Three-Staged, and Interdigitated TVCs. Calculations were performed using the (a) Standard, (b) RNG, and (c) Realizable k-ε RANS turbulence models.

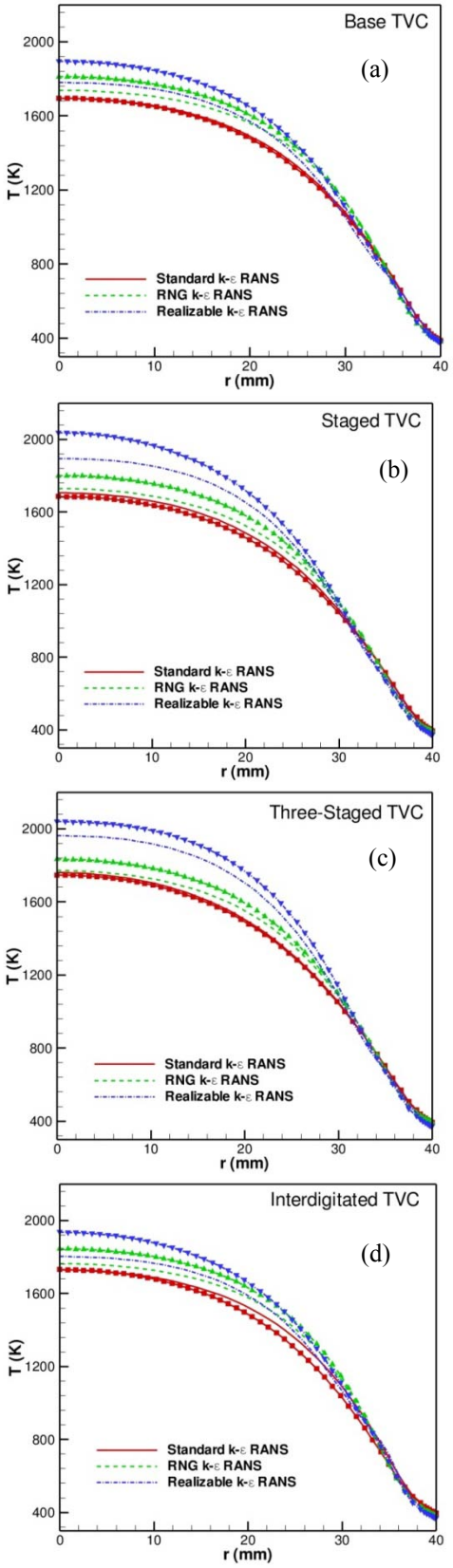

Figure 10. Outlet radial temperature profiles for the non-swirled (lines) and swirled (lines and symbols) (a) Base, (b)

Staged, (c) Three-Staged, and (d) Interdigitated TVCs. Calculations were performed using the Standard, RNG, and Realizable k-ε RANS turbulence models.

D. EFFECT OF FUEL AND AIR JETS AND HEAT RELEASE ON THE FLOW CHARACTERISTICS OF THE STAGED TRAPPED VORTEX COMBUSTOR

Figure 11 presents the velocity flow field for the Staged TVC (a) without fuel and air jets, (b) with fuel and air jets but without combustion, (c) only with back (or second) cavity fuel and air jets, and (d) only with front (or first) cavity fuel and air jets. Figure 12 reports their drag coefficients. Without any fuel and air jets, obviously, there is no combustion and both cavities exhibit backflow. In this section we used this case as the baseline for comparison unless otherwise mentioned. The first cavity exhibits two vortices. The outermost vortex has edge velocities in the direction of the mainstream and the innermost vortex has edge velocities in opposite direction. Therefore, the flow regime is that of WBF (cf. Figure 4). On the other hand, the second cavity exhibits a single dominating vortex that does not fit well in the cavity with edge velocities in the same direction as the mainstream. Therefore, this cavity exhibits characteristics of both WBF and UCV regimes (cf Figure 4). The total drag coefficient for this configuration is 0.55 with 0.33 and 0.22 corresponding to pressure and viscous drag, respectively. The total drag coefficient of the first cavity is 0.6, whereas that for the second cavity is -0.1. The reason why the first cavity has higher drag is because the first cavity exhibits WBF flow structure, whereas the second one exhibits WBF/UCV flow structure.

For the case with the fuel and air jets but without combustion the flow structure of both the first and second cavity remain somewhat similar to that without jets (i.e. WBF in first cavity and WBF/UCV in second cavity). However, the effect of the jets is to increase the total drag coefficient from 0.55 to 0.7 with 0.47 and 0.23 (cf. Figure 12) corresponding to pressure and viscous drag, respectively. Backflow still occurs in both cavities. The total drag coefficient of the first cavity is still 0.6, whereas that of the second cavity is 0.01 (cf. Figure 12).

With only the jets of the second cavity turned on the total drag coefficient increases from 0.55 to 1.45 with 1.15 and 0.3 (cf. Figure 12) corresponding to pressure and viscous drag coefficients, respectively. Nevertheless, this is a total drag reduction of 23 % when compared with the Staged TVC of Figure 5 (cf. Figure 6). This decrease might be due to either a decrease on ϕ_{GBL} or achievement of a more stable flame. Moreover, the flow dynamics of the first cavity has changed drastically when compared with the Staged TVC of Figure 5. Because fuel and air jets of the first cavity are turned off two counter-rotating vortices are formed like in the case without jets and the case with jets but without combustion. There is also substantial backflow that was not observed in the Staged TVC of Figure 5. This backflow transports the hot products from the second cavity to the first cavity. The first cavity drag coefficient drops from 0.68 to 0.6 corresponding to now 41 % of total drag and 52 % of pressure drag in comparison with the Staged TVC of Figure 5 (cf. Figure 6 and Figure 12). The second cavity drag coefficient remains constant at 0.03. The major reduction on pressure drag comes from the downstream face of the second disk (i.e. 80% reduction in pressure drag). The first cavity corresponds to only 20 % reduction in pressure drag.

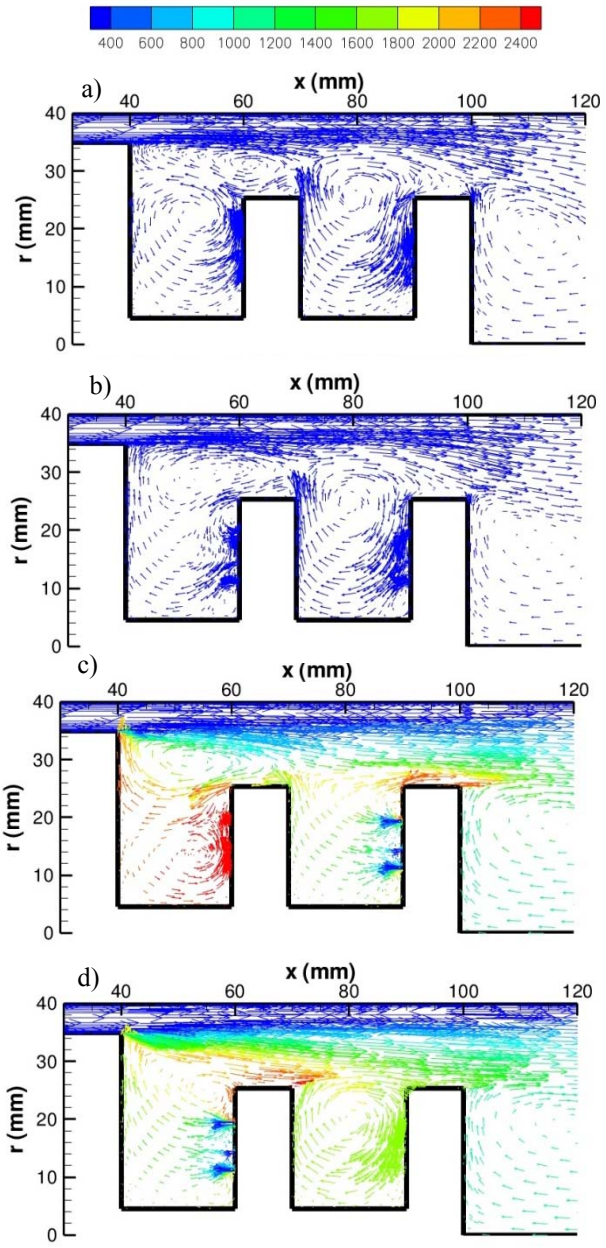

Figure 11. Velocity vectors for the Staged TVC (a) without fuel and air jets, (b) with fuel and air jet but without combustion, (c) only with front (or first) cavity fuel and air jets, and (d) only with back (or second) cavity fuel and air jets. The calculations were performed using the RNG k-ε RANS model. The velocity vector lengths are scaled with magnitude and colored with temperature in Kelvin.

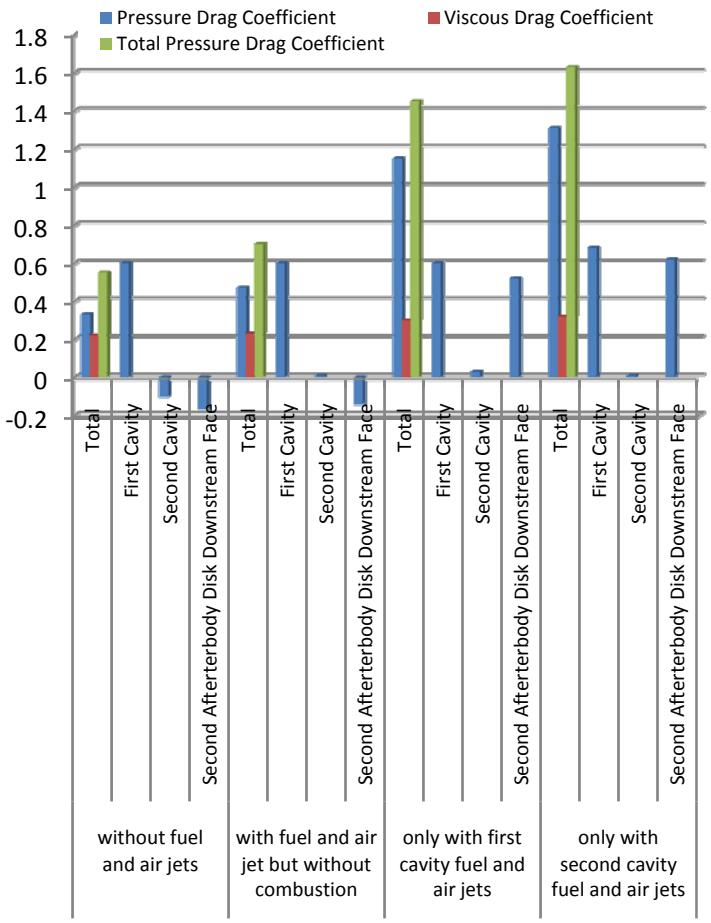

Figure 12. Pressure, viscous and total drag coefficients as well as individual pressure drag coefficients of the multiple components of the Staged TVC discussed in the context of Figure 11.

With only the jets of the first cavity the total drag coefficient increase from 0.55 to 1.63 with 1.31 and 0.32 corresponding to pressure and viscous drag (cf. Figure 12), respectively. Nonetheless, this is a total decrease of 14 % when compared to the Staged TVC of Figure 5 (cf. Figure 6). In terms of reducing drag, it is more effective to use only the jets of the second cavity. The flow dynamics of the second cavity has changed drastically when compared with the Staged TVC of Figure 5. Because fuel and air jets in the second cavity are turned off one single vortex with edge velocity vectors in the same direction as the mainstream flow is formed. The structure resembles that of the SCV (cf. Figure 4). The dominating vortex does not seem to fit very well in the cavity because its center is slightly shifted radially from the center of the cavity. In comparison with the Staged TVC of Figure 5, the first cavity drag coefficient remains constant at 0.68 (cf. Figure 12) corresponding to 41 % of total drag and 52 % of total pressure drag. The second cavity drag coefficient is small (~ 0.01). The largest reduction of pressure drag comes from the downstream face of the second disk (i.e. 92% reduction in pressure loss). The 8% reduction comes from the second cavity.

The temperature exit profiles of the two reactive Staged TVCs presented in Figure 11 are nearly identical as illustrated in Figure 13. Therefore, it appears to be more advantages to use only second (back) cavity jets instead of only first (front) cavity jets because the latter provides parabolic temperature profile with lower drag. This figure also shows that by turning either set of jets the maximum temperature at the exit is also lowered.

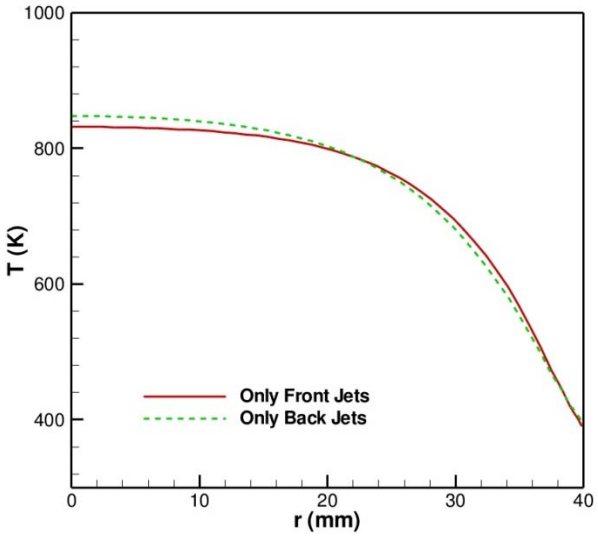

Figure 13. Outlet radial temperature profiles for the non-swirled Staged TVC with only front fuel and air jets and with only back fuel and air jets. Calculations were performed using the RNG k-ε RANS turbulence model.

4. IMPLICATIONS FOR THE INTER-TURBINE BURNER DESIGN

Based on the results of multi-cavity TVCs engineer/designer/modeler would need to use two consecutive cavities to reduce drag or pressure losses. For instance, two radial vane cavities (RVC) on the curved radial vane (CRV) or two consecutive cavity-in cavities (CIC) on the circumferential cavity (CC) could potentially reduce pressure losses (or drag) without altering the existing exit temperature profile. Note that, if two consecutive CIC are used in the ITB, fuel and air jets should only be injected through the downstream CIC (based on the swirl flow direction). This injection also needs to be either facing radially inward or in the same direction of the swirl flow in order to avoid reheating of the upstream cavity as in Figure 11. Moreover, another design strategy for the ITB could be to have two consecutive concentric CC in which only fuel and air is injected from the downstream CC (based on the mainstream flow direction). The injection should be radially inward or in the same direction of the mainstream to avoid accumulation of hot products in the other CC. Furthermore, modeling and simulation should be done with either RNG or Realizable k-ε RANS turbulence models when swirl flows are present and never with the Standard version. In the design of the ITB it

should be taken into account that the swirl will increase the exit temperature profile.

5. CONCLUSIONS

An extensive computational investigation on the characteristics of these multi-cavity TVCs is presented. FLUENT is used for modeling the axisymmetric reacting flow past cavities using a global eddy dissipation mechanism for C_3H_8-air combustion and detailed thermodynamic and transport properties. Calculations are performed using Standard, RNG, and Realizable k-ε RANS turbulence models. The numerical results are validated against experimental temperature measurements on the Base TVC. The volume of this combustor and the amount of fuel and air injection in this cavity is represented in three different layouts of splitting the volume and the air and fuel flow rates proportionally to match the volume of the Base TVC and thus four combustors are studied: Base, Staged, Three-Staged, and Interdigitated. Important conclusions are the following:

1. Results indicate that the pressure drag, representing the total pressure loss is the major contributor to total drag for all combustors. However, viscous drag is still significant. With the Staged TVC the pressure drag decreases, whereas the viscous drag remains nearly constant. With the Three-Staged TVC the total drag does not further decrease and both pressure and viscous drag contributions do not change. On the other hand, with the Interdigitated TVC the pressure drag increases from that of the Base TVC while the viscous drag slightly decreases.
2. For all multi-cavity TVCs pressure drag is pronounced in the most upstream cavity and very low in any other cavity. Large pressure drag is also observed in the downstream face of the most downstream afterbody disk, as that of Refs. 22 and 23.
3. The effect of adding swirl flow is to increase the fuel-air mixing and as a result to maximize the exit temperature by enhancing mixing of the hot products with the mainstream cold air. This increase in temperature is not capture by the Standard model and, consequently, it should not be use for modeling the three-dimensional ITB. Moreover, in descending order the Realizable predicts higher temperature than the RNG and Standard models.
4. The jets and heat release contribute to increase pressure drag with the former being greater. In addition, the cavity flow structure is modified.
5. By turning off the fuel and air jets in the Staged TVC lower drag (or pressure loss) and exit temperature are achieved. It is more effective to turn off the fuel and air jets in the front cavity in order to reduce pressure losses.

ACKNOWLEDGMENTS

This material is based on research sponsored by U.S. Air Force Research Laboratory under agreement number F33615-03-2-2347. The authors are thankful to Joseph Zelina of AFRL/RZTC, WPAFB, Hugh Thornburg of Mississippi State University and to Viswanath Katta and Jack Yoder of ISSI, Inc. for their help with frequent technical consultations during the preparation of this paper. The views and conclusions contained herein are those of the authors and should not be interpreted as necessarily representing the official policies or endorsements, either expressed or implied, of U.S. Air Force Research Laboratory or the U.S. Government.

REFERENCES

1. Zelina, J., Sturgess,G. J., and Shouse, D. T., "The Behavior of an Ultra-compact Combustor (UCC) Based on Centrifugally-Enhanced Turbulent Burning Rates," 40th AIAA/ASME/SAE/ASEE Joint Propulsion Conference and Exhibit, AIAA Paper 2004-3541, 2004.
2. Greenwood, R. T., Anthenien, R. A., and Zelina, J., "Computational Analysis of the Ultra Compact Combustor," 43rd AIAA Aerospace Sciences Meeting and Exhibit, AIAA Paper 2005-220, 2005.
3. Çengel, Y.A., Boles, M.A., Thermodynamic: An Engineering Approach, McGraw Hill, 2002.
4. Lin, C-X, Sekar, B., Zelina, J., Holder, R.J., Thornburg, H., "Numerical Simulation of Inter-turbine Burner (ITB) Flows with the Inclusion of V-Gutter Flame Holders," Proceedings of ASME Turbo Expo 2008: Power for Land, Sea, and Air, GT2008-50337.
5. Anderson, W.S., Radtke, J.T., King, P.I., Thornburg, H., Zelina, J., Sekar, B., " Effects of Main Swirl Direction on High-g Combustion," 44th AIAA/ASME/SAE/ASEE Joint Propulsion Conference & Exhibit, 21-23 July 2008, Hartford, CT., AIAA2008-4954, 2008.
6. Thornburg, H., Sekar, B., Zelina, J., Greenwood, R., "Numerical Study of an Inter-turbine (ITB) Concept with Curved Radial Vane," 45th AIAA Aerospace Sciences Meeting & Exhibit, Reno, NV, AIAA Paper 2007-649.
7. Thornburg, H.J., Sekar, B., Zelina, J., "Analysis of Curved Radial Vane Cavity Arrangements for Inter-turbine Burner," 46th AIAA Aerospace Sciences Meeting & Exhibit, Reno, NV, AIAA Paper 2008-1024.
8. Thornburg, H.J., Sekar, B., Zelina, J., Lin, C.-X., Holder, R.J., "Prediction of Inter-Turbine Burner (ITB) Performance with Curved Radial Vane Cavity at Various Equivalence Ratios," Proceedings of ASME Turbo Expo 2008: Power for Land, Sea, and Air, GT2008-50192.
9. Sekar, B., Thornburg, H., Lin, C.-X., Holder, R.J., Zelina, J., "Inter-turbine Burner (ITB) Performance with Circumferential Cavity Volume Variations for Cold and Heated Fuel Injection," 44th AIAA/ASME/SAE/ASEE Joint Propulsion Conference & Exhibit, Hartford, CT. AIAA Paper 2008-4566.

10. Zelina, J., Shouse, D. T., and Hancock, R. D., "Ultra-Compact Combustors for Advanced Gas Turbine Engines," ASME IGTI 2004-GT-53155.

11. Lefebvre, A.H., Gas Turbine Combustion, Taylor&Francis, 1983.

12. Mawid, M.A., Park, T.A., Thornburg, H., Sekar, B., Zelina, J., "Numerical Analysis of Inter-turbine Burner (ITB) concepts for Improved Gas Turbine Engine Performance," 43rd AIAA Aerospace Science Meeting & Exhibit, Reno, NV, AIAA Paper 2005-1162.

13. Katta, V.R., Roquemore, W.M., "Numerical Studies on Trapped-vortex Concepts for Stable Combustion," Trans. ASME J. Eng. Gas Turbines Power 120 (1998) 60-68.

14. Little Jr., B.H., Whipkey, R.R., "Locked Vortex Afterbodies," J. Aircraft 16 (1979) 296-302.

15. Katta, V.R., Roquemore, W.M., "Numerical Studies on Trapped-vortex Concepts for Stable Combustion," Trans. ASME J. Eng. Gas Turbines Power 120 (1998) 60-68.

16. Katta, V.R., Roquemore, W.M., "Numerical Studies of Trapped-vortex Combustor," 32nd AIAA/ASME/SAE/ASEE/ Joint Propulsion Conference & Exhibit, AIAA-1996-2660, Lake Buena Vista, FL.

17. Zdanski, P.S.B., Ortega, M.A., Fico Jr., N.G.C.R., "On the Flow over Cavities of Large Aspect Ratio: A Physical Analysis," Int. J. Heat Mass Trnsfr. 22 (2006) 458-466.

18. Zdanski, P.S.B., Ortega, M.A., Fico Jr., N.G.C.R., "Numerical Study of the Flow over Shallow Cavities," Comp. & Fluids 32 (2003) 953-974.

19. D'yanchenko, A.Y., Terekhov, V.I., Yarygina, N.I., "Vortex Formation and Heat Transfer in Turbulent Flow Past a Transverse Cavity with Inclined Frontal and Rear Walls," Int. J. Heat & Mass Trnsfr. 51 (2008) 3275-3286..

20. Puranam, S., Arici, J., Sarzi-Amade, N., Dunn-Rankin, D., Sirignano, "Turbulent Combustion in a Curving, Contracting Channel with a Cavity Stablized Flame, Proc. Combust. Institute 32 (2009) 2973-2981.

21. Briones, A.M., Zelina, J., Katta, V.R., "Flame Stabilization in Small Cavities," AIAA J. (48) 2010, 224-235.

22. Mair, W.R., "The Effect of a Rear-mounted Disc on the Drag of a Blunt-based Body of Revolution," The Aeronautical Quarterly, Nov. 1965, 350-360.

23. Molki, M. Faghri, M., "Interaction between a Buoyancy-driven Flow and an Array of Annular Cavities," Sadhana 19 (5) 705-721.

24. Holmes, D.G., Connell, S.D., "Solution of the 2D Navier-Stokes Equation on Unstructured Adaptive Grids," AIAA 9th Computational Fluid Dynamics Conference, June, 1989.

25. Bird, R.B., Stewart, W.E., Lightfoot, E.N., Transport Phenomena, Wiley, New York , 1960.

26. Reid, R.C., Prausnitz, J.M., Poling, B.E., The properties of gases and liquids, McGraw-Hill, New York, 1987.

27. Chu, W.-W., Yang, V., Majdalani, J., "Premixed Flame Response to Acoustic Waves in a Porous-walled Chamber with Surface Mass Injection," Combust. Flame 133 (2003) 359-370.

28. Ansys, Inc., "Ansys Fluent 12.0 Theory Guide", www.fluent.com.

29. Kee, R.J., Rupley, F.M., Miller, J.A., Coltrin, M.E., Grcar, J.F., Meeks, E. Moffat, H.K., Lutz, A.E., Dixon-Lewis, G., Smooke, M.D., Warnatz, J., Evans, G.H., Larson,, R.S., Mitchell, R.E., Petzold, L.R., Reynolds, W.C., Caracotsios, M., Stewart, W.E., Glarborg, P., Wang, C., McLellan, C.L., Adigun, O., Houf, W.G., Chou, C.P., Miller, S.F., Ho, P., Young, P.D., Young, D.J., Hodgson, D.W., Petrova, M.V., Puduppakkam, K.V., Chemkin Release 4.1.1, Reaction Design, San Diego, CA (2007).

30. Al-Midani, O.M., "Preliminary Design of Liquid Bipropellant Microfabricated Rocket Engine," M.S. Thesis, Massachusetts Institute of Technology, 1998.

31. Kader, B., "Temperature and Concentration Profiles in Fully Turbulent Boundary Layers," Int. J. Heat Mass Transfer, 24(9):1541-1544, 1981.

32. Hsu, K. Y., Goss, L. P., Trump, D. D., and Roquemore, W. M., "Performance of a Trapped-Vortex Combustor," AIAA Paper 95-0810, Washington, D. C, Jan. 9-12, 1995.

33. Quaale, R.J., Anthenien, R.A., Zelina, J., Ehret, J., "Flow Measurements within a High Swirl Ultra Compact Combustor for Gas Turbine Engines," ISABE-2003-1141.